Lawrence Berkeley Laboratory
UNIVERSITY OF CALIFORNIA

Materials & Molecular Research Division

Submitted to Advances in Ceramics

TRANSFORMATION TOUGHENING IN CERAMICS

A.G. Evans, D.B. Marshall, and N.H. Burlingame

December 1980

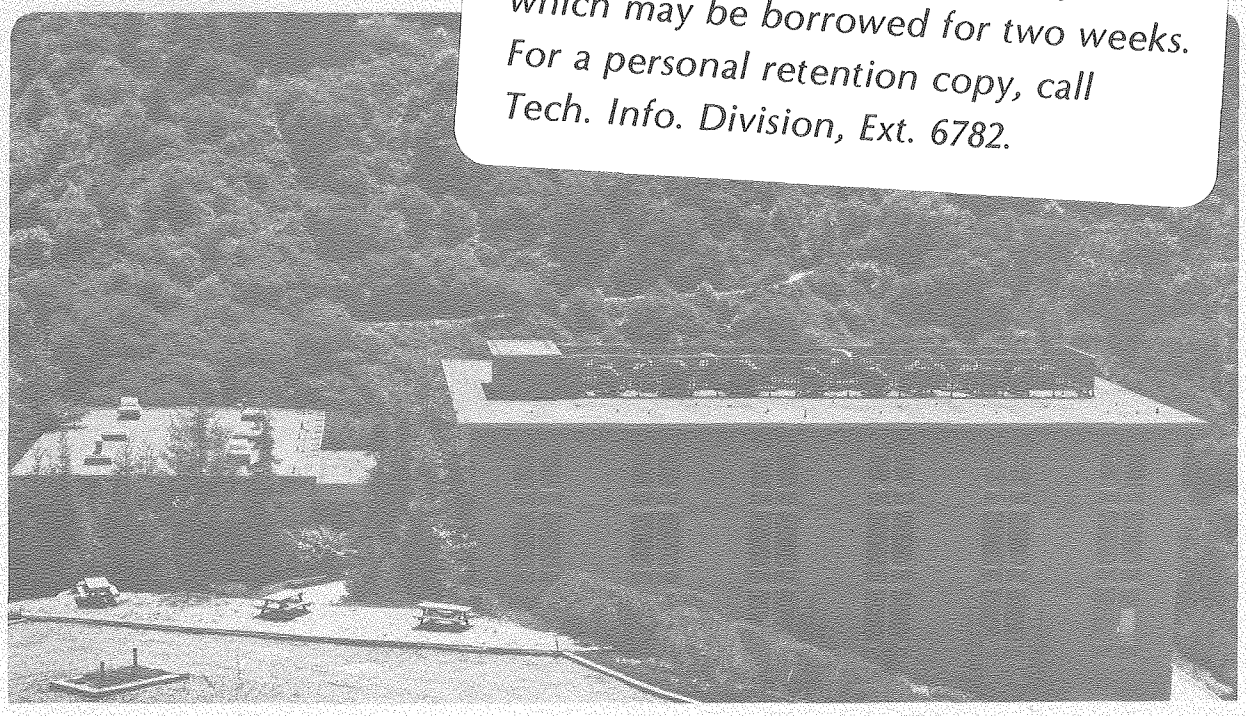

Prepared for the U.S. Department of Energy under Contract W-7405-ENG-48

DISCLAIMER

TRANSFORMATION TOUGHENING IN CERAMICS

by

A. G. Evans, D. B. Marshall and N. H. Burlingame

Materials and Molecular Research Division, Lawrence Berkeley Laboratory
and Department of Materials Science and Mineral
Engineering, University of California
Berkeley, CA 94720

ABSTRACT

The origin of transformation toughening in ceramics is examined using two separate approaches: one based on the stress field ahead of the crack and the other on the changes in thermodynamic potential during a crack increment. Both approaches yield essentially similar predictions of trends in toughness with particle size, temperature, composition, etc. The stress intensity analysis provides fully quantitative predictions of the toughness. These indicate that the shielding of the crack by the transformation zone only develops in the presence of a transformed wake, leading to R-curve behavior.

This work was supported by the Director, Office of Energy Research, Office of Basic Energy Sciences, Materials Science Division of the U.S. Department of Energy under Contract No. W-7405-ENG-48.

1. INTRODUCTION

The enhancement of toughness in ceramics achieved through the controlled use of martensitic transformation mechanisms has emerged as a major research interest[1-9], with considerable practical potential. The development of toughness requires relatively stringent control of composition and microstructure[3,4,6,9]. An ability to interpret and predict the microstructure/composition that provides the optimum toughness is thus an important aspect of the development and control of toughened materials. This capability must be based on a micromechanics model that contains the correct physical characteristics of the toughening process. The presently available models provide, in some instances, conflicting predictions of the role of microstructure and temperature on the toughness[6,7,9]. The intent of this paper is to provide physically consistent analyses of toughening, based on the best available knowledge of the mechanisms involved in the development of toughness.

Toughening occurs through the development of a zone of transformed material ('process zone') around the crack tip (fig. 1a). This process zone is a source of stress and displacement disturbance that tends to shield the crack tip from the applied stress, in a manner analagous to a plastic zone. The toughening is thus related to the dimensions of the process zone and the amplitude of the disturbance, through a crack extension criterion. The mechanics associated with the crack tip stresses and the crack surface displacements are the basis of pertinent crack extension criteria.

Alternatively, fracture can be analysed by examining the energy changes that accompany crack extension. This approach contains inherent uncertainties associated with the modes of energy dissipation. But, the energy analysis, upon comparision with the mechanics analysis, may provide some useful additional insights into the mechanism of toughening.

An essential aspect of the toughening magnitude is the dimension of the transformation zone. The prediction of this zone dimension is a complex problem. The analysis should be based upon a critical stress amplitude $\left(p^A_{ij}\right)_c$ for transformation (analagous to a critical shear stress condition for estimating the plastic zone size and shape). However, independent experimental estimates of $\left(p^A_{ij}\right)_c$ (c.f. the yield strength for plasticity) are difficult to obtain and hence, are not yet available. The results obtained from a simplified analysis, based upon the interaction energy for an isolated particle in a uniform stress field[6,7], will be discussed.

2. TOUGHNESS/ZONE SIZE RELATIONS

The influence of a transformation zone on the fracture toughness resides in the modified stress field or crack opening displacement induced by the zone. The modified stress field for a stress/strain behavior typical of transformation (fig. 1b) exhibits the characteristics depicted in fig. 1c. There is a reduction in the near tip field characterized by a local value of the stress intensity factor, K_I^{local}; the remote field (for a small transformation zone) is dictated by the applied stress intensity factor, K_I^{∞} ; and there is an intermediate region of relatively invariant stress, with a magnitude determined by the transformation strain. Fracture is determined by either the local or the intermediate stress field, as dictated by the

specific crack extension mechanism. Fracture in most ceramics (those that are not subject to microcracking) is generally considered to occur by the direct advance of the crack tip[10]. This mechanism is assumed in the present analysis. Whereupon, the increment in toughness can be deduced directly from the change in K_I^{local} induced by the transformation zone. However, situations in which fracture initiates in the intermediate zone should not be discounted.

A convenient procedure for calculating the stress intensity factor change induced by a process zone is illustrated in fig. 2a. The process zone is allowed to undergo an unconstrained transformation strain, e^{T*}. A stress σ_{ij}^W is then applied to the zone to restore it to its original dimensions. Equal and opposite tractions

$$T_j^W = n_i \sigma_{ij}^W \tag{1}$$

where n_i is the boundary normal, are then applied to the zone boundary to achieve stress continuity in the system. These tractions induce a change in stress intensity, characterised by the stress intensity factor[11]

$$\Delta K_I^T = \frac{1}{2\sqrt{2\pi}(1-\nu)} \int \underset{\sim}{T}^W \cdot \underset{\sim}{h} \, dS \tag{2}$$

where dS is an element of the zone boundary and h is a weight function. Referring to the axes X_1 and X_2 and the coordinates (r, θ) depicted in fig. 1b, the following relations pertain;

$$T_1^W = \sigma_{11}{}^W \cos\Psi + \sigma_{12}{}^W \sin\Psi$$

$$T_2^W = \sigma_{12}{}^W \cos\Psi + \sigma_{22}{}^W \sin\Psi$$

$$\left.\begin{aligned} h_1 &= \frac{\cos(\theta/2)}{\sqrt{r}}\left[2\nu-1+\sin(\theta/2)\sin(3\theta/2)\right] \\ h_2 &= \frac{\sin(\theta/2)}{\sqrt{r}}\left[2-2\nu-\cos(\theta/2)\cos(3\theta/2)\right] \end{aligned}\right\} \quad (r<<a) \qquad (3)$$

where Ψ relates the zone surface normal to the reference axis (fig 2b).

Initially, the only macroscopic particle transformation strain is considered to be the dilational component e^T. The zone restoring stress is then a uniform hydrostatic compression p, independent of zone shape, particle orientation, shape, etc. The change in stress intensity determined (in accord with the above procedure) from the transformation volume strain is found to be a function of the zone geometry selected for the analysis[12]. Specifically, zones contained ahead of the crack tip (fig. 3a) do not generally result in a signficant reduction in the the local stress intensity; whereas, zones that extend over the crack surface (fig. 3b) provide substantial crack shielding. The transformed wake thus appears to be the predominant source of toughening. Most toughness measurements pertain to cracks which, upon introduction into the system, create a continuous zone over the crack surface (fig. 3b), and the full toughening should thus be experienced. However, when a prior zone over the crack does not exist, crack growth should be characterized by an R-curve, as schematically illustrated in fig. 3c. This issue is discussed more extensively in the Appendix.

These toughness characteristics are demonstrated by conducting calculations of the local stress intensity for two zone profiles: one fully contained ahead of the crack (fig. 3a), and the other of uniform width extending fully over the crack surface (fig. 3b). Firstly, consider a zone contour suggested by the dilational crack tip field (fig. 3a);

$$r = r^* \cos^2(\theta/2) \tag{4}$$

where r^*, the zone dimension at $\theta = 0$, is a function of the applied stress intensity factor, K_I^∞ ,

$$r^* = \frac{2(1+\nu)^2}{9\pi} \left(\frac{K_I^\infty}{p_c^A} \right)^2 \tag{5}$$

Noting the following relations

$$dS = (r^*/\sqrt{2}) \, [1 + \cos\theta]^{1/2} \, d\theta$$

$$\cos\Psi = [\cos\theta + \cos 2\theta]/\sqrt{2} \, (1 + \cos\theta)^{1/2}$$

$$\sin\Psi = [\sin\theta + \sin 2\theta]/\sqrt{2} \, (1 + \cos\theta)^{1/2}$$

the stress intensity change becomes;

$$\frac{\Delta K_I^T}{p\sqrt{r^*}} = \frac{1}{8\sqrt{2\pi}(1-\nu)} \int_{-\pi}^{+\pi} [(\sin\theta + \sin 2\theta)(4-4\nu- \cos\theta - \cos 2\theta) \tan(\theta/2) + (\cos\theta + \cos 2\theta)(4\nu - 2 + \cos\theta - \cos 2\theta)] \, d\theta$$

$$= 0 \tag{6}$$

The absence of crack tip shielding is thus manifest for this zone profile.

Secondly, consider a transformation zone of uniform width r_o[†]. The crack is subject to a uniform compression p due to restoration of the zone to its initial (pre-transformation) shape, and to tractions, $-p$, acting at the zone boundary (fig. 3b) that establish stress continuity. The change in stress intensity factor attributed to the application of these forces, obtained by employing the requisite point force functions, is given by[12];

[†]The zone width r_o is related to the zone dimension ahead of the crack r^*, by $r_o = (\sqrt{3}/2)^2 r^*$.

$$\frac{\Delta K_I^T}{p\sqrt{r_o}} = -1.13 + \frac{0.28}{(1-\nu)} + 0.094\,\frac{(1+4\nu)}{(1-\nu)} \qquad (7)$$

where the first term derives from the uniform compression, the second term from the tractions over the zone surface (up to the crack tip) and the third term from the tractions from the zone ahead of the crack†. For a typical value of Poisson's ratio, $\nu = 1/4$, eqn. (7) becomes

$$\frac{\Delta K_I^T}{p\sqrt{r_o}} = -0.51 \qquad (8)$$

The negative character of ΔK_I^T confirms that the zone induces crack shielding.

It now remains to determine the magnitude of the traction p, in order to deduce the toughening induced by the transformation zone. For plane strain conditions, p is related to the volume strain and the concentration of particles in the zone;

$$p = \kappa \Delta V V_f$$

where ΔV is the unconstrained transformation volume strain of an individual particle, V_f is the volume concentration of particles and κ is the average bulk modulus. The change in stress intensity factor thus becomes,

$$\frac{\Delta K_I^T}{V_f E \Delta V \sqrt{r_o}} = \frac{1}{3(1-2\nu)}\left[-1.13 + \frac{0.28}{(1-\nu)} + 0.094\,\frac{(1+4\nu)}{(1-\nu)}\right] \qquad (10)$$

†This result exhibits some dependence on the precise shape selected for the zone ahead of the crack[16]. The shape used to obtain eqn. (7) was determined by assuming a constant zone radius, r_o, ahead of the crack.

which for $\nu = 1/4$ becomes;

$$\frac{\Delta K_I^T}{V_f E \Delta V \sqrt{r_o}} = -0.34 \qquad (11)$$

Fracture is assumed to proceed when the local stress intensity factor attains the fracture resistance of the pre-transformed material†, K_{IC}^M (a quantity that depends upon the volume fraction of particles);

$$K_I^{local} \equiv K_I^\infty + \Delta K_I^T = K_{IC}^M \qquad (12)$$

The level of the applied stress intensity factor at the criticality is thus,

$$K_{IC}^\infty = K_{IC}^M + 0.34 V_f E \Delta V \sqrt{r_o} \qquad (13)$$

An analagous treatment of the influence of the macroscopic transformation shear strain is substantially more complex, because of the vector nature of the shear strain, i.e. the particle shape and orientation distributions become important considerations. Each analysis thus requires specific information about the particles and the transformation morphologies. Such analyses are evidently of merit only for materials in which the dilational transformation strain does not afford the principal contribution to the toughening.

The relative influence of the volume strain and the shear strain can be conveniently estimated by comparing the predictions derived from eqn. (13) with experimental results. Suitable results exist for the MgO/PSZ studied

†The toughening described in this section is relative to the toughness of the overaged material, which contains the influence of local interactions between the transformed particles and the crack, e.g. crack deflection effects.

by Porter and Heuer[4] and by Schoenlein[13]. The appropriate measurements are: $r_o \approx 0.6\mu m$, $\Delta V \approx 0.058$[3], $E \sim 2 \times 10^{11} Pa$, $V_f \sim 0.3$. The toughness ratio is thus predicted from eqn. (13) to be, $K_{IC}^{\infty}/K_{IC}^{M} = 1.4 \pm 0.1$. This compares with a measured toughening for the same material condition of $\sim 1.6 \pm 0.2$. The volume strain thus appears to be the major source of toughening in this instance. Further studies are evidently needed to establish the detailed dependence of toughness on the volume strain and the macroscopic shear strain.

3. THE TRANSFORMATION ZONE SIZE

Prediction of the transformation zone dimension requires a detailed knowledge of the nucleation of the stress induced transformation. The specific nucleation mechanisms pertinent to ceramics, such as ZrO_2, have not been identified. An upper bound solution based on the net change in thermodynamic potential is thus presented, and its use justified by comparison with zone size observations.

Zone profile observations[14] generally indicate characteristics expected from a dilation dominated transformation, i.e. a zone extending ahead of the crack tip[6]. Hence, for present purposes, it is considered that the particles exhibit insignificant macroscopic transformation shear strain and that the transformation is activated by the hydrostatic component of the stress. The change in thermodynamic potential upon transformation has been determined for transformations in which entropy changes (other than those associated with the chemical free energy change of the particle) are neglected[7];

$$\frac{\Delta\phi}{(4/3)\pi R^3} = -\Delta F_o + \Gamma_T/d + 3\Delta\Gamma_i/R + 0.15E\Delta V^2 - p^A\Delta V + 0.13E\gamma_T^2 (1.2 + R/d)^{-1} \quad (14)$$

where R is the particle radius, d is the twin (variant) spacing, ΔF_o is the chemical free energy change, Γ_T is the twin boundary energy, $\Delta\Gamma_i$ is the change in interface energy and γ_T is the twinning (variant) shear strain. If the twin boundary energy and the change in interface energy are small, the lower bound stress needed to induce transformation ($\Delta\phi = 0$) becomes;

$$p_c^A/E\Delta V = 0.15 - \Delta F_o/E\Delta V^2 + 0.13(\gamma_T/\Delta V)^2 (1.2 + R/d)^{-1} \quad (15)$$

Substituting the lower bound critical stress into eqn. (5), the corresponding upper bound transformation zone size at the criticality becomes;

$$r_o \approx \frac{1}{4\pi}\left(\frac{K_{IC}^{\infty}}{E\Delta V}\right)^2 \frac{1}{[0.15 - \Delta F_o/E\Delta V^2 + 0.13(\gamma_T/\Delta V)^2(1.2 + R/d)^{-1}]^2} \quad (16)$$

A comparison of eqn. (16) with transformation zone size observations in PSZ indicates a predicted zone size less than twice the measured value[7]. This is similar to predictions of the plastic zone size based upon the linear elastic approximation. The nucleation barrier does not appear, therefore, to dominate the crack tip transformation in PSZ. The upper bound zone size estimate should thus be an approximation suitable for anticipating toughness trends.

Toughening characteristics can be identified by inserting the zone width from eqn. (16) into eqn. (13) to give;

$$1 - \frac{K_{IC}^{M}}{K_{IC}^{\infty}} = \frac{0.7V_f}{[1 - 7\Delta F_o/E\Delta V^2 + (\gamma_T/\Delta V)^2 (1.2 + R/d)^{-1}]} \qquad (17)$$

This result is similar in general form to that found in previous studies[6,7]. The qualitative implications for effects of temperature, composition, etc. on the toughening are thus essentially unchanged by the present analysis.

4. THERMODYNAMIC CONSIDERATIONS

The toughening induced by a martensite transformation can also be estimated from considerations of the changes in thermodynamic potential that accompany an increment in crack length[6,7,9]. It has already been demonstrated[6] that, since the stress state near the crack tip remains essentially unchanged during a crack increment, the net energy change associated with the transformation can be considered as the energy difference between untransformed particles remote from the crack tip (subject to the remotely applied stress) and transformed particles placed over the crack surface (subject to zero stress), as illustrated in fig. 4. For this problem, when the particles are stress free prior to transformation, the toughness is given by[7];

$$\mathcal{G}_I^{\infty} = \mathcal{G}_{IC}^{M} + [V_f r_o/(4/3)\pi R^3]\left(\Delta\phi|_{p^A=0}\right)$$

$$= \mathcal{G}_{IC}^{M} + E\Delta V^2 r_o V_f [0.15 - \Delta F_o/E\Delta V^2 + 0.13 (\gamma_T/\Delta V)^2 (1.2 + R/d)^{-1}] \qquad (18)$$

Introducing the zone size from eqn. (16) the toughness becomes

$$1 - \frac{\mathcal{J}_{IC}^{M}}{\mathcal{J}_{IC}^{\infty}} = \frac{0.6V_f}{[1 - 7\Delta F_o/E\Delta V^2 + (\gamma_T/\Delta V)^2 (1.2 + R/d)^{-1}} \qquad (19)$$

The final result is remarkably similar to that derived from the modified crack tip stress field (eqn. 17). This may be fortuitous because in both instances an upper bound thermodynamic criterion for the zone dimension has been employed to attain the final toughening expression. Nevertheless, it is of considerable interest to note that the thermodynamic result in its present form also anticipates the trends with zone profile identified from the stress intensification analysis. Notably, a zone contained ahead of the crack does not produce significant toughening; the increase in toughness is only manifest when the zone extends over the crack surface (Appendix).

The location of the energy changes during a crack increment are also of interest. The criterion selected for zone formation requires that the change in thermodynamic potential in the newly created zone (fig. 5) be zero. The increase in potential attributed to the transformation zone (to be supplied by the enchanced $(\mathcal{J})$ must occur, therefore, in other segments of the zone. The principal source of the increase in potential is the increase in elastic energy that occurs at particles over the crack surface, as the stress on the particles is released by the crack advance (fig. 5). The change in potential has a magnitude comparable to the interaction energy (with the local stress), and must be a positive quantity because the tension on the particles (which reduces the elastic energy) is being reduced in this region.

5. PARTICLE SIZE DISTRIBUTION EFFECT

The toughness should evidently exhibit some dependence on the particle size distribution, through the size dependent adjacence to the critical particle size R_c for stress free transformation. The problem can be addressed by firstly determining the zone tractions for each small particle size range, R to R + dR (within the distribution, f(R)dR), deducing the resultant ΔK_I^T, and then summing over all untransformed particles within the distribution. This procedure yields the following relation for the toughening

$$1 - \frac{K_{IC}^M}{K_{IC}^\infty} = \frac{V_f}{(7\Delta F_o/E\Delta V^2 - 1)\langle R^3\rangle} \int_{\sim d}^{\hat{R}} \frac{R^3(1.2d+R)}{(R_c-R)} f(R)dR \qquad (20)$$

The lower limit, d , is selected because it is improbable that small particles near the crack tip will transform into a single twin (variant)[7]. The upper bound is determined by the level of the remotely applied strain relative to the transformation strain[15]. Normalization of the integral in eqn. (20) gives;

$$1 - \frac{K_{IC}^M}{K_{IC}} = \frac{V_f R_c^3}{(7\Delta F_o/E\Delta V^2 - 1)\langle R^3\rangle} \int_{\sim 2/\eta_c}^{\hat{R}/R_c} \frac{z^3(z+2.4/\eta_c)}{(1-z)} f(z, R_o/R_c, k)dz \qquad (21)$$

where R_o is the scale parameter and k the shape parameter for the particle size distribution and η_c is the number of twins in a particle of critical size. Some typical results obtained by assuming an extreme value

function for $f(R)dR$ are plotted in fig. 6. Comparison with eqn. (17) indicates that the size distribution introduces an upper bound toughness. The level of the upper bound decreases as the variance increases. However, no additional variables are introduced.

The particle size distribution is also related to the ratio λ of the monoclinic phase content to the total content of ZrO_2 through the critical size R_c ,

$$\lambda = [1/\langle R^3 \rangle] \int_{R_c}^{\infty} R^3 f(R) dr \qquad (22)$$

There are thus unique relations between the predicted toughness and the monoclinic phase content for each value of the shape parameter k . The predictions of toughness as a function of monoclinic phase content should be directly comparable with experimental results.

6. CONCLUSIONS

Analyses of transformation toughening have been presented that permit the interpretation of toughness results in various ceramic systems, and allow trends in the toughness with the important internal and external variables to be predicted. Preliminary comparisons between the predictions and results for partially stabilised zirconia indicate that the toughening derives primarily from the volume strain of transformation, once the transformation zone dimension has been prescribed. However, the transformation shear strain (as manifest in the twin or variant structure of the martensite) could be important in determining the transformation zone dimension. This topic requires further study.

The analyses also suggest the existence of R-curve behavior when the cracks in the material are not accompanied by a pre-existent transformation zone. This behavior resides in the observation that crack tip shielding only initiates when the tranformation zone extends over the crack surface.

The trends in toughness with the important variables predicted by the present analyses are similar to those anticipated by previous studies. Specifically, important influences of temperature, chemical composition, particle size distribution, matrix toughness and the transformation strain are predicted, in accord with experimental observations.

ACKNOWLEDGMENT

This work was supported by the Director, Office of Energy Research, Office of Basic Energy Sciences, Materials Science Division of the U.S. Department of Energy under Contract No. W-7405-ENG-48.

APPENDIX

AN ESTIMATE OF R-CURVE BEHAVIOR

The detailed characteristics of R-curves for transformation toughened ceramics can be determined by either of the two approaches used in this paper. These details will be presented in a subsequent publication. An approximate evaluation is described here, in order to illustrate the range of crack entension over which the principal increase in crack growth resistance is established. The thermodynamic approach is used for this purpose.

Commence with an initial stress free crack without a transformation zone. Application of an external loading causes a transformation zone to develop and the crack tip advances from A to B (fig. 7a), leaving an intervening wake. The energy changes that accompany an additional increment, da , in crack length then relate to the value of $\mathcal{G}_{IC}$ at crack extension AB: $\mathcal{G}_{IC} = \mathcal{G}^{\circ}_{IC} + \Delta\mathcal{G}_{IC}$, where $\mathcal{G}^{\circ}_{IC}\,da = 2\Gamma da$ is the increase in surface energy, and $\Delta\mathcal{G}_{IC}da$ is the increase in potential associated with the transformed particles. Consider the changes in potential that occur in a strip of width dy (fig.7b). The total potential within this strip, for unit specimen thickness, is

$$\phi(y) = V_f dy \int_0^{\infty} \phi_y(x)dx \qquad (A1)$$

where x is the coordinate along the crack plane (fig. 7a) and $\phi_y(x)$ is the potential per unit volume at x . The change in potential following transformation is

$$\Delta\phi = -\Delta F_o + \Delta\phi_o - \Delta\phi_{int} \qquad (A2)$$

where $\Delta\phi_o$ is the stress free elastic energy and $\Delta\phi_{int}$ is the interaction energy with the local stress p. Then, if the zone boundary is defined by the thermodynamic condition, $\Delta\phi = 0$, the change in $\phi(y)$ during the crack advance, given by the shaded area in fig. 7b, is

$$\frac{d\phi(y)}{da} = \Delta\phi^{\circ}_{int} - \Delta\phi^{A}_{int} \tag{A3}$$

where $\Delta\phi^{\circ}_{int}$ and $\Delta\phi^{A}_{int}$ are the magnitudes of the interaction energy at the front and rear boundaries of the transformation zone. The increase in crack growth resistance is then,

$$\Delta\mathcal{J}_{IC} = V_f \int_{-r_o}^{r_o} (\Delta\phi^{\circ}_{int} - \Delta\phi^{A}_{int})dy \tag{A4}$$

In the absence of a wake, $\Delta\phi^{\circ}_{int} = \Delta\phi^{A}_{int}$ and there is no increase in toughness. For a fully developed wake, $\Delta\phi^{A}_{int} = 0$, and the maximum toughness increase pertains;

$$\Delta\hat{\mathcal{J}}_{IC} = 2V_f\, r_o \Delta\phi^{\circ}_{int} \tag{A5}$$

which is the result quoted in the text (with $\Delta\phi = 0$ at the zone boundary). For intermediate conditions, the trend can be estimated by computing the stress over the rear boundary and deducing the interaction energy from

$$\Delta\phi^{A}_{int} = p^{A} e^{T} \tag{A6}$$

The final result is;

$$\Delta\mathcal{J}_{IC} = \Delta\hat{\mathcal{J}}_{IC}\left[1 - \frac{\beta\sqrt{(\alpha/r_o) + \sqrt{(\alpha/r_o)^2 + 1}}}{3^{3/4}\sqrt{(\alpha/r_o)^2 + 1}}\right]$$

where $\Delta a = r_o \tan 30 - \alpha$ is the crack extension and β is a constant

between 1 and 2. This result is plotted in fig. 7c (for $\beta = 2$). It is noted that ΔJ_{IC} attains an essentially invariant level when the crack advance is about 3 to 4 times the zone height. Hence, for small zones, this varying crack extension resistance will have little influence upon the mechanical behavior of transformation toughened materials. Important effects will only emerge when the zone size is a significant fraction ($\gtrsim 0.1$) of the crack length.

REFERENCES

1. R. C. Garvie, R. H. Hanninck and R. T. Pascoe, Nature 258 (1975) 703.
2. N. Claussen, Jnl. Amer. Ceram. Soc. 59 (1976) 49.
3. R. H. Hanninck, Jnl. Mater. Sci. 13 (1978) 2487.
4. D. L. Porter and A. H. Heuer, Jnl. Amer. Ceram. Soc. 60 (1977) 183.
5. D. L. Porter, A. G. Evans and A. H. Heuer, Acta Met. 27 (1979) 1649.
6. A. G. Evans and A. H. Heuer, Jnl. Amer. Ceram. Soc. 63 (1980) 241.
7. A. G. Evans, N. Burlingame, M. Drory and W. M. Kriven, Acta Met., in press.
8. T. K. Gupta, F. F. Lange and J. H. Bechtold, Jnl. Mat. Sci. 13 (1978) 1464.
9. F. F. Lange, Science Center Report SC 5117.6TR (Oct 1979)
10. A. G. Evans, D. L. Porter and A. H. Heuer, 'Fracture 1977' (Ed. D. M. Taplin), Univ. Waterloo Press, vol. 1 (1977) p.
11. P. C. Paris, R. McMeeking and S. Tada, ASTM STP 601 (1978).
12. J. Hutchinson, R. McMeeking and A. G. Evans, to be published.
13. L. Schoenlein, M.S.Thesis, Case Western Reserve University (1979).
14. M. Ruhle, to be published.
15. A. G. Evans and K. T. Faber, Jnl. Amer. Ceram. Soc., in press.
16. D. B. Marshall, M. Drory and A. G. Evans, to be published.

FIGURE CAPTIONS

Fig. 1. a. A schematic of a process zone around a crack induced by the martensitic transformation of particles.

b. A typical stress, strain behavior for a martensite transformation; e^T_{ij} is the transformation strain, $\left(p^A_{ij}\right)_c$ is the critical stress needed to induce transformation (which depends on particle size, etc.). Note the linearity of the stress/strain relation for stresses in excess of the transformation stress.

c. The modified stress ahead of a crack tip in the presence of of a transformation zone.

Fig. 2. a. The unconstrained and constrained process zones, indicating the tractions needed to maintain stress continuity.

b. The coordinate system used to conduct the stress intensity analysis.

Fig. 3. a. A process zone contained ahead of the crack tip, with the hydrostatic contour. ΔK for this zone is zero.

b. A process zone contained over the crack surface. This zone provides crack tip shielding.

c. A schematic of R-curve behavior for transformation toughening in an annealed material.

Fig. 4. A schematic indicating that the increased crack growth resistance emanates from the difference in thermodynamic potential of an untransformed region within the applied field (remote from the tip) and a transformed region over the crack surface where the stress level is essentially zero.

Fig. 5. A schematic indicating the regions of the process zone in which the changes in thermodynamic potential occur during a crack increment.

Fig. 6. Predictions of toughening as a function of particle size for several particle size distributions.

Fig. 7. The R-curve determined by employing a thermodynamic treatment

a. The zone characteristics.

b. The potential change during a crack increment.

c. The relative toughening during a crack advance.

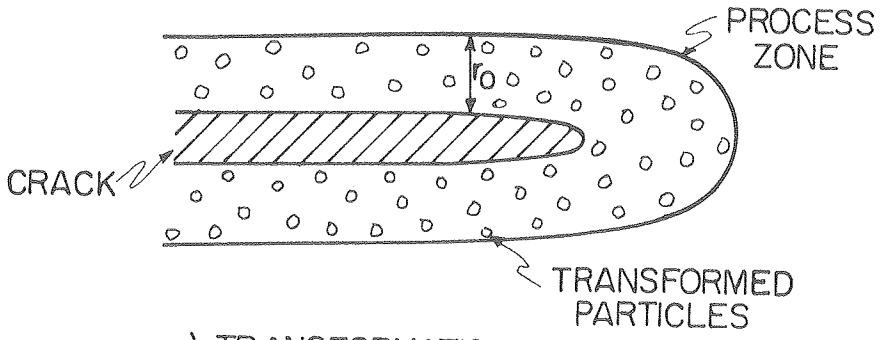

a) TRANSFORMATION ZONE

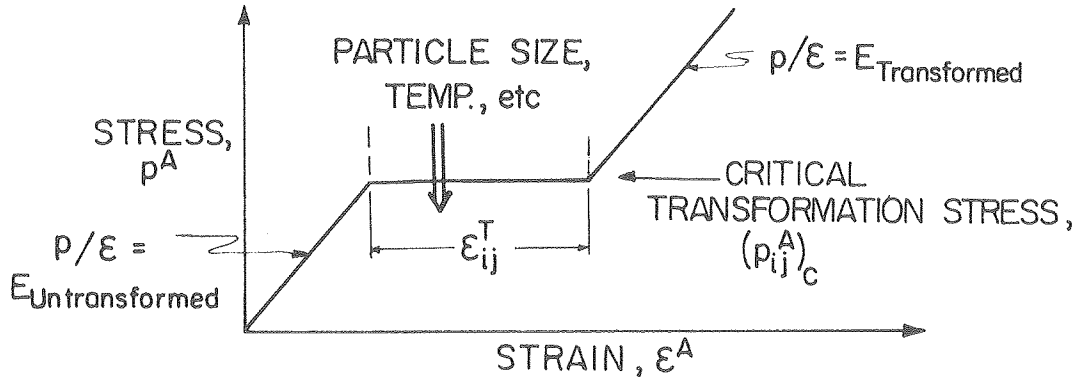

b) A TYPICAL STRESS, STRAIN BEHAVIOUR FOR A MARTENSITIC TRANSFORMATION

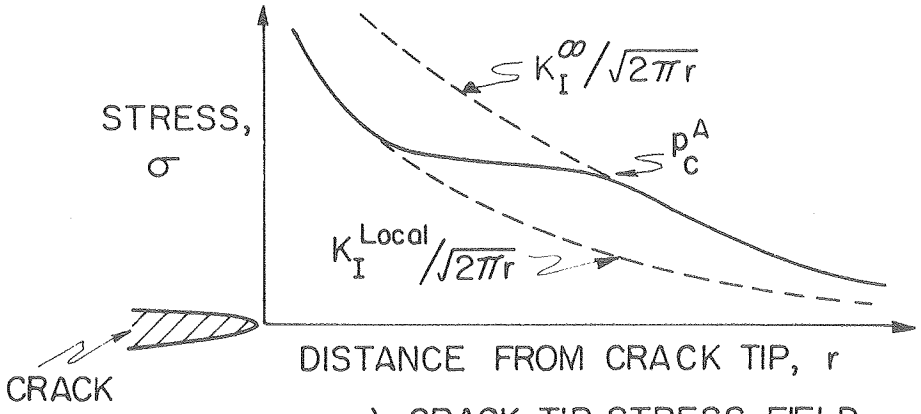

c) CRACK TIP STRESS FIELD

XBL809-5930

Fig. 1

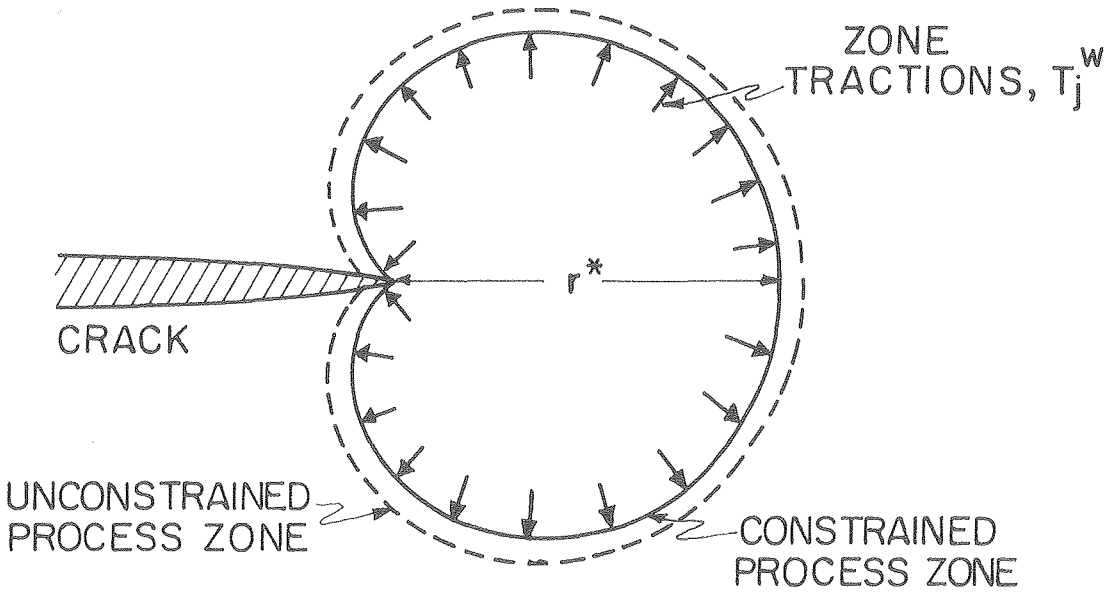

a) THE ZONE TRACTIONS T_j^w

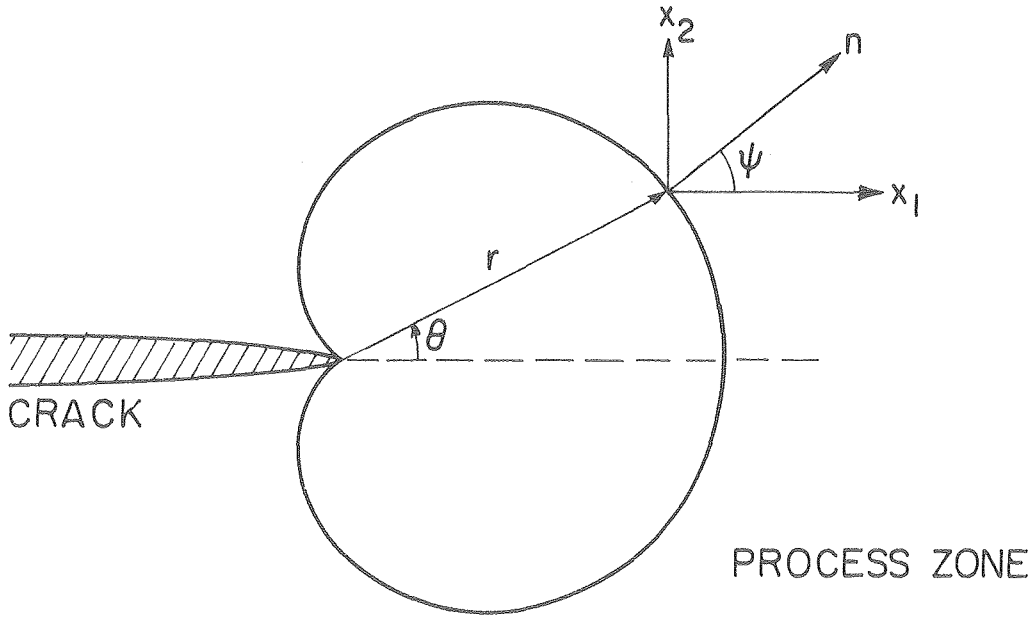

b) COORDINATES OF STRESS INTENSITY ANALYSIS

XBL809-5931

Fig. 2

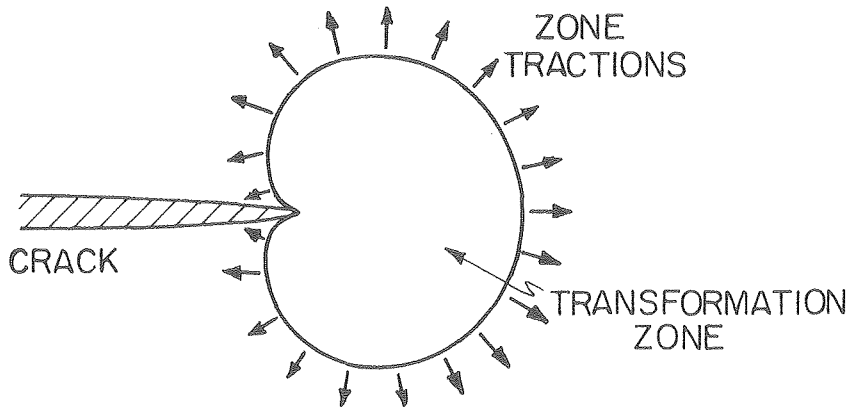

a) ZONE CONTAINED AHEAD OF CRACK TIP

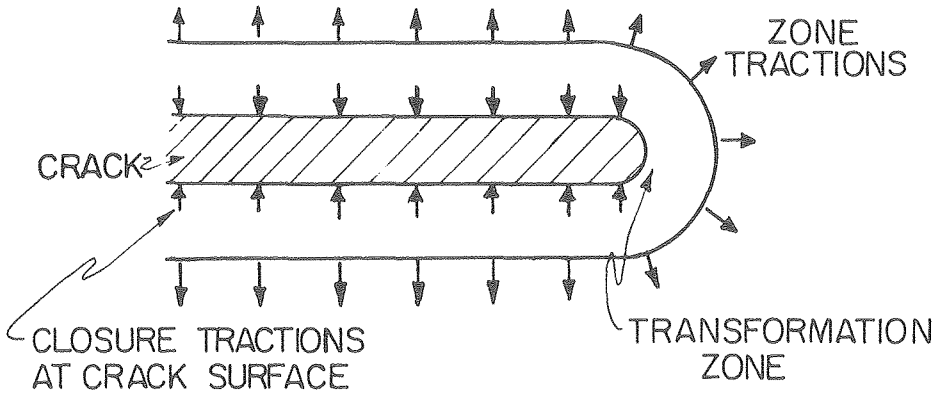

b) ZONE OF UNIFORM WIDTH OVER CRACK SURFACE

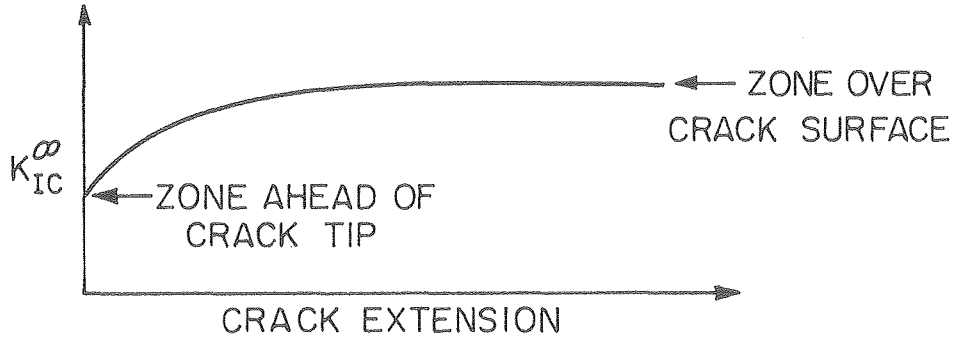

c) SCHEMATIC R-CURVE BEHAVIOUR

XBL809-5932

Fig. 3

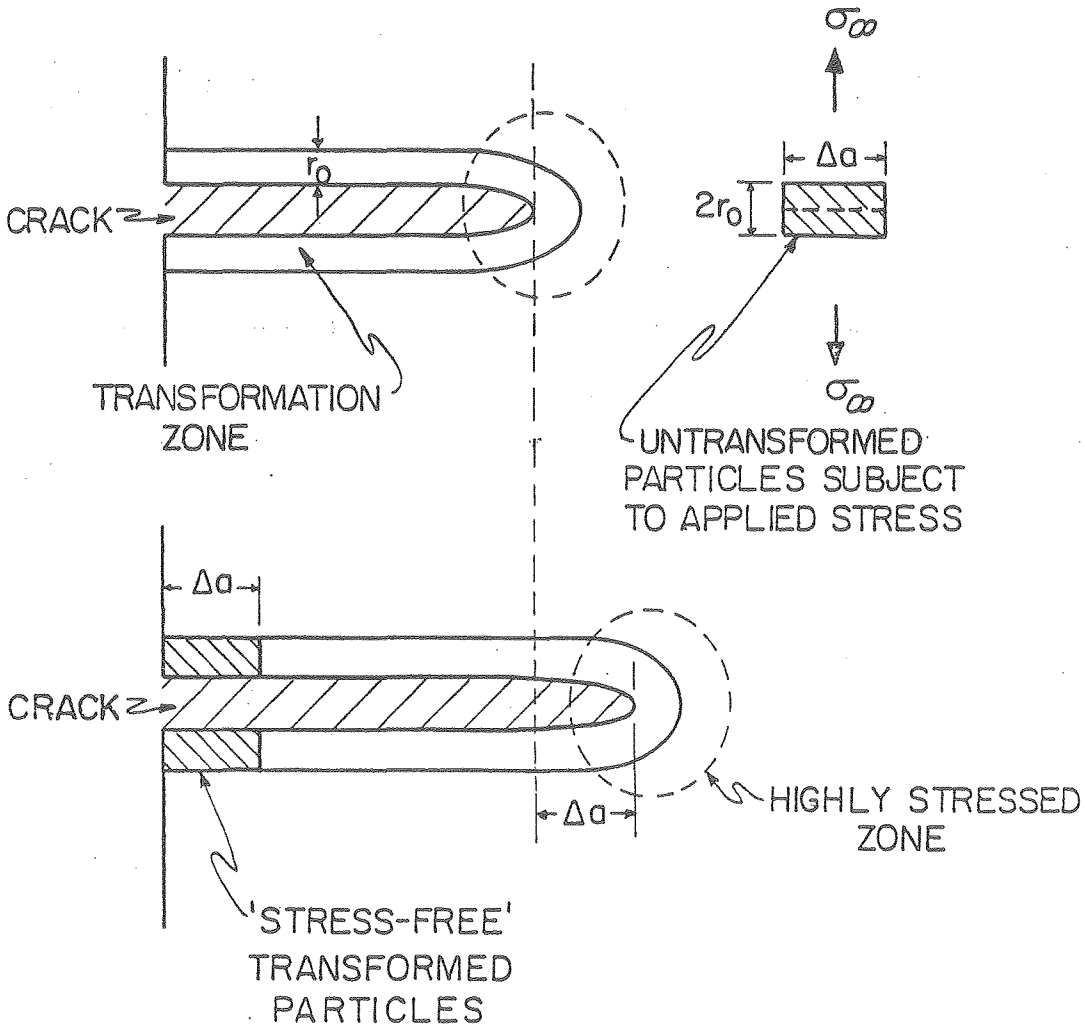

XBL 809-5933

Fig. 4

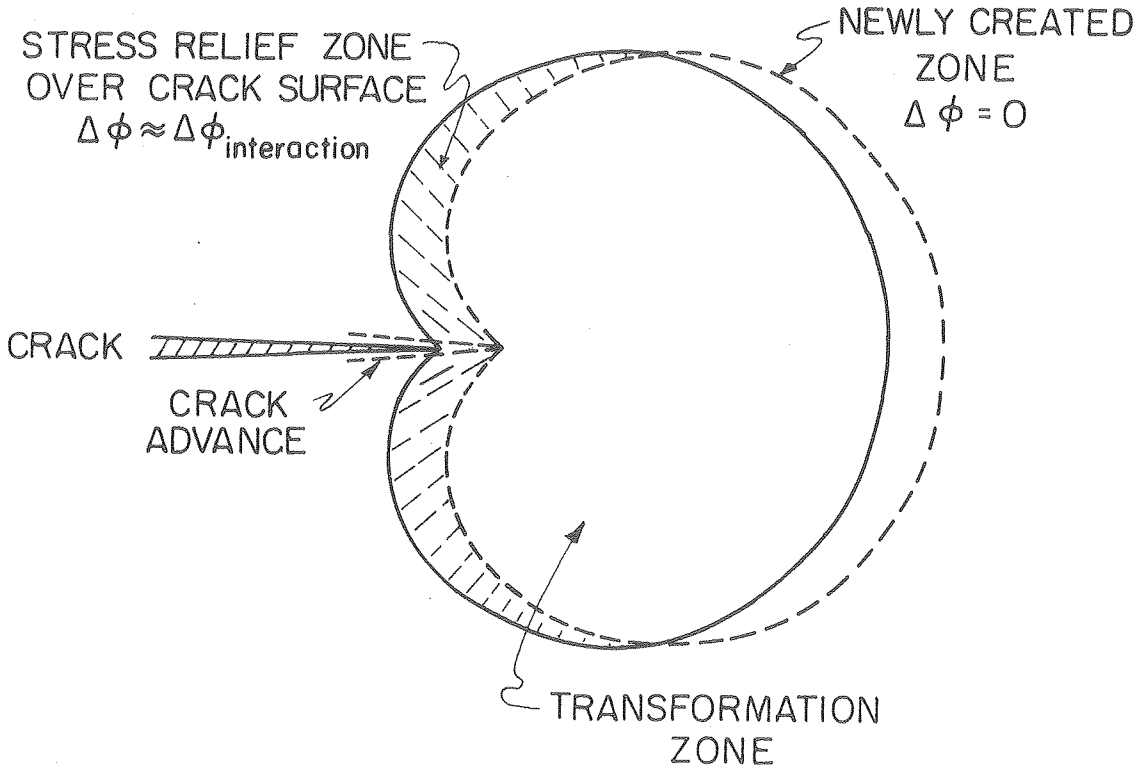
STRESS RELIEF ZONE
OVER CRACK SURFACE
$\Delta\phi \approx \Delta\phi_{interaction}$
NEWLY CREATED
ZONE
$\Delta\phi = 0$
CRACK
CRACK
ADVANCE
TRANSFORMATION
ZONE
XBL 809-5934

Fig. 5

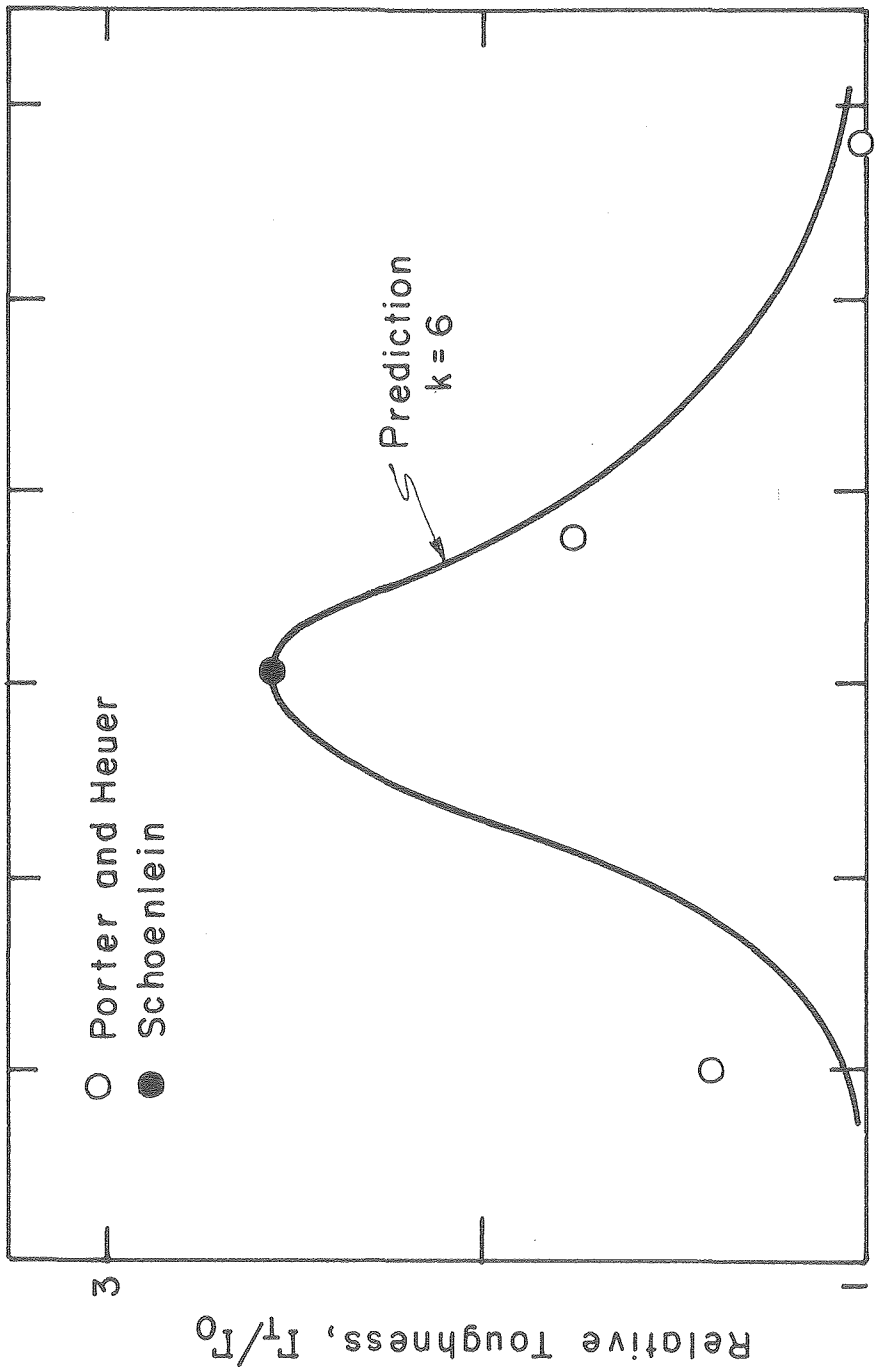
Relative Toughness, Γ_T/Γ_O
3
1
0.4
0.6
0.8
1.0
1.2
1.4
1.6
Relative Particle Size, $a/\hat{a}$
O Porter and Heuer
● Schoenlein
Prediction
k=6
XBL 801-4541

Fig. 6

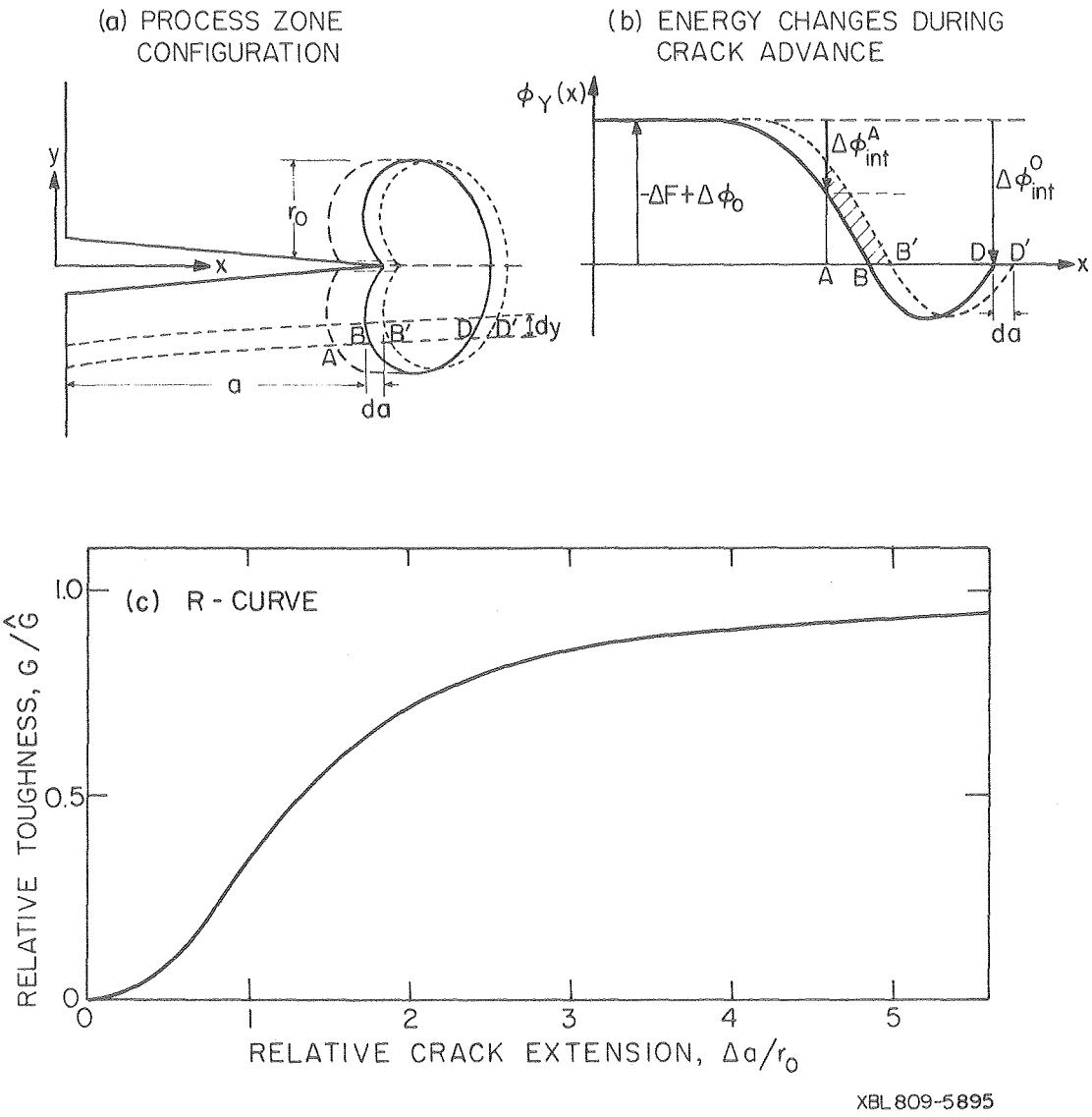
(a) PROCESS ZONE CONFIGURATION
(b) ENERGY CHANGES DURING CRACK ADVANCE
y
x
r_o
A
B
B′
D
D′
dy
a
da
$\phi_Y(x)$
$-\Delta F+\Delta\phi_o$
$\Delta\phi^A_{int}$
$\Delta\phi^o_{int}$
(c) R - CURVE
RELATIVE TOUGHNESS, $G/\hat{G}$
RELATIVE CRACK EXTENSION, $\Delta a/r_o$
0
0.5
1.0
1
2
3
4
5
XBL 809-5895

Fig. 7